Monthly Notices
of the
ROYAL ASTRONOMICAL SOCIETY

MNRAS **468,** L21–L25 (2017) doi:10.1093/mnrasl/slx019

Direct evidence for Lyα depletion in the protocluster core

Rhythm Shimakawa,[1,2⋆] Tadayuki Kodama,[1,2] Masao Hayashi,[2] Ichi Tanaka,[3] Yuichi Matsuda,[1,2] Nobunari Kashikawa,[1,2] Takatoshi Shibuya,[4] Ken-ichi Tadaki,[5] Yusei Koyama,[1,3] Tomoko L. Suzuki[1,2] and Moegi Yamamoto[1]

[1]*Department of Astronomical Science, SOKENDAI, Osawa, Mitaka, Tokyo 181-8588, Japan*
[2]*National Astronomical Observatory of Japan, Osawa, Mitaka, Tokyo 181-8588, Japan*
[3]*Subaru Telescope, National Astronomical Observatory of Japan, 650 North A'ohoku Place, Hilo, HI 96720, USA*
[4]*Institute for Cosmic Ray Research, The University of Tokyo, 5-1-5 Kashiwanoha, Kashiwa, Chiba 277-8582, Japan*
[5]*Max-Planck-Institut für Extraterrestrische Physik, Giessenbachstrasse, D-85748 Garching, Germany*

Accepted 2017 January 31. Received 2017 January 18; in original form 2016 December 22

ABSTRACT

We have carried out panoramic Lyα narrow-band imaging with Suprime-Cam on Subaru towards the known protocluster USS1558−003 at $z = 2.53$. Our previous narrow-band imaging in the near-infrared identified multiple dense groups of Hα emitters (HAEs) within the protocluster. We have now identified the large-scale structures across a ∼50 comoving Mpc scale traced by Lyα emitters (LAEs) in which the protocluster traced by the HAEs is embedded. On a smaller scale, however, there are remarkably few LAEs in the regions of HAE overdensities. Moreover, the stacking analyses of the images show that HAEs in higher-density regions show systematically lower escape fractions of Lyα photons than those of HAEs in lower-density regions. These phenomena may be driven by the extra depletion of Lyα emission lines along our line of sight by more intervening cold circumgalactic/intergalactic medium and/or dust in the dense core. We also caution that all the previous high-z protocluster surveys using LAEs as tracers would have largely missed galaxies in the very dense cores of the protoclusters where we would expect to see any early environmental effects.

Key words: galaxies: evolution – galaxies: formation – galaxies: high-redshift.

1 INTRODUCTION

High-z galaxy protoclusters (Sunyaev & Zeldovich 1972) are ideal test beds where we can understand how cluster galaxies form and grow during the course of cosmic mass-assembly history and the build-up of large-scale structures (LSSs) in the Universe (White & Frenk 1991; Cole et al. 2000). They directly inform us of what is occurring in the early phase of cluster formation and galaxy formation, which then tells us what the physical mechanisms are that lead to the galaxy diversity that depends on the environment, as seen in the local Universe (Dressler 1980; Cappellari et al. 2011).

The observational limitation due to the Earth's atmosphere has created a gulf between high-z galaxy surveys at $z < 2.6$ and those at $z > 2.6$. At redshifts greater than 2.6, the bright Hαλ6565 emission line is no longer observable from ground-based telescopes, and the Lyαλ1216 line is the most commonly used spectral feature of star-forming galaxies that can be captured by optical instruments. This technique has been widely used to identify galaxies at high redshifts, both in the general fields and in overdense regions, such as protoclusters (Ouchi et al. 2003; Venemans et al. 2007). However, we know that only a small fraction of star-forming galaxies show detectable Lyα emission lines (Hayes et al. 2010; Matthee et al. 2016; Hathi et al. 2016). Furthermore, the environmental dependence of Lyα emitters (LAEs) has largely been unexplored. Therefore, understanding the dependence of physical properties and the selection effects of LAEs across various environments is strongly desired.

In this respect, the dual emitter surveys of Hα emitters (HAEs) and LAEs for the known protoclusters at $z = 2.1$–2.6 can play a key role in testing the Lyα selection effect in a high-z protocluster search. This letter studies Lyα emissivities of Hα-emitting galaxies in a known dense protocluster, USS 1558−003, at $z = 2.53$ ($\alpha_{J2000} = 16^{h}01^{m}17^{s}$ $\delta_{J2000} = -00^{\circ}28'47''$, hereafter USS 1558) discovered by Kajisawa et al. (2006), Kodama et al. (2007) and Hayashi et al. (2012) with MOIRCS on the Subaru telescope. Our recent deep Hα narrow-band survey of this region succeeded in detecting more protocluster members, amounting to 100 HAEs in total (Hayashi et al. 2016), allowing us to characterize sub-structures such as clumps associated with USS 1558. Given such a unique laboratory of an overdense environment at $z = 2.5$, we manufactured a dedicated narrow-band filter for this specific target and installed it on the Suprime-Cam so that we can also target LAEs associated

⋆ E-mail: rhythm.shimakawa@nao.ac.jp

© 2017 The Authors
Published by Oxford University Press on behalf of the Royal Astronomical Society

Downloaded from https://academic.oup.com/mnrasl/article/468/1/L21/3060937 by guest on 10 April 2024

with this region. Also, the wider field of view of Suprime-Cam (32 × 27 arcmin) compared to MOIRCS (7 × 4 arcmin) enables us to map LSSs in and around USS 1558.

We assume the cosmological parameters $\Omega_M = 0.3$, $\Omega_\Lambda = 0.7$ and $h = 0.7$ and we employ a Chabrier (2003) stellar initial mass function and the AB magnitude system (Oke & Gunn 1983) throughout this letter. Galactic extinctions for NB428 and the *B* band are assumed to be 0.55 and 0.57 mag, respectively (Schlegel, Finkbeiner & Davis 1998; Fitzpatrick 1999; Schlafly & Finkbeiner 2011).[1]

2 OBSERVATION AND DATA ANALYSES

We performed Lyα line imaging of USS 1558 at $z = 2.53$ with the Subaru Prime Focus Camera (Suprime-Cam; Miyazaki et al. 2002) on the Subaru telescope. We used the custom-made narrow-band filter NB428, which has a central wavelength of 4297 Å and full width at half-maximum (FWHM) of 84 Å. This is designed so that the filter FWHM neatly captures the Lyα lines at $z = 2.53 \pm 0.03$ (emission or absorption) from HAEs at $z = 2.52 \pm 0.02$ associated with the USS 1558 protocluster selected by the narrow-band filter, NB2315, installed on MOIRCS/Subaru (see Shimakawa et al. 2017a).[2] The combined analysis of a resonant Lyα line by NB428 and a non-resonant Hα line by NB2315 enables us to make the first systematic comparison of the spatial distributions between LAEs and HAEs, and to investigate the environmental dependence of the Lyα photon escape fractions within the protocluster.

The observation was executed on 2015 June 10 under a photometric condition but with relatively bad seeing (FWHM = 0.8–1.4 arcsec). The science frames with seeing sizes worse than 1.3 arcsec were trashed and we used 19 frames of 700 s exposures each, amounting to 3.7 h of net integration time in total. The data were reduced in exactly the same way as in Shimakawa et al. (2017a) based on a data reduction package for the Suprime-Cam, SDFRED (ver. 2; Yagi et al. 2002; Ouchi et al. 2004). The pipeline includes the standard procedures. Sky subtraction was conducted with a mesh size of 13 arcsec. We additionally implemented cosmic ray reduction using the algorithm L.A.Cosmic (van Dokkum et al. 2011). The final combined image has a seeing size of FWHM = 1.24 arcsec and a limiting magnitude of 25.15 mag at 5σ with 2.5 arcsec aperture diameter accounting for galactic extinction.

Combining the reduced NB428 data with the existing counterpart *B* band image ($B_{5\sigma} = 25.72$ mag with 2.5 arcsec aperture diameter) provided by Hayashi et al. (2016), we select LAE candidates in the same manner as in Shimakawa et al. (2017a). Here, the seeing FWHM of the *B* band is tuned to that of the NB428 image. The object photometry is performed by SEXTRACTOR (ver. 2.19.5; Bertin & Arnouts 1996). Photometric measurements are done in double-image mode using the narrow-band image for source detections, and we employed aperture photometries with 2.5 arcsec diameter. This work imposes selection criteria as follows: (1) the narrow-band flux excess is greater than 3σ with respect to the photometric error,

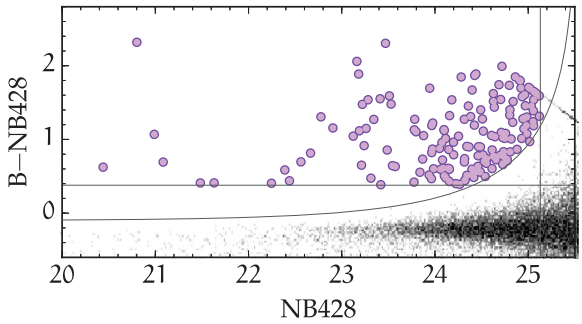

Figure 1. Colour–magnitude diagram. The black shows the NB-detected sources. The purple circles indicate narrow-band emitters that meet our criteria: (1) the line EW is greater than 15 Å in the rest frame (horizontal line), (2) the line flux excess is larger than 3σ (black curve) and (3) the detection at NB428 is more than the 5σ level (vertical line).

(2) the Lyα equivalent width (EW) is higher than $EW_{Ly\alpha} = 15$ Å in the rest frame and (3) $NB_{5\sigma} < 25.13$ mag. The correction factor for the colour term (i.e. the zero-point of $B - NB$) is assumed to be -0.1, which is tailored to that in our previous study of another field using the same NB428 filter (Shimakawa et al. 2017a). 2σ limiting magnitudes are assumed for the sources with *B*-band detection levels lower than 2σ.

As a result, in total 162 objects satisfied our selection criteria (Fig. 1). This letter employs these samples as LAE candidates at $z = 2.5$. However, note that a considerable number of foreground contaminations, such as [O II]$\lambda\lambda$3727, 3730 and C IV$\lambda\lambda$1548, 1551, may be included even though we are targeting the region that hosts the known protocluster (cf. ∼60 per cent in the random field according to Sobral et al. 2017). The currently available photometric data that cover the entire field are only the *B*, *r* and *z* band photometries with Suprime-Cam, which are not sufficient to decontaminate our LAE samples cleanly. This caution should be kept in mind when our LAE samples are discussed.

3 RESULTS

Fig. 2 a shows the spatial distribution of the LAE candidates over the entire field of Suprime-Cam. The protocluster cores traced by the HAEs with MOIRCS in our previous studies (Hayashi et al. 2012, 2016) are embedded in the much larger-scale structures traced by LAEs. Hayashi et al. (2016) identified 100 HAEs based on the combined technique of using the narrow-band selection and two colour–colour diagrams (r′JKs and r′H_{F160W}Ks). These samples are limited to the star-formation rates (SFRs) of $>2.2\ M_\odot\ yr^{-1}$ without dust correction. 41 of those HAEs have been spectroscopically confirmed by Shimakawa et al. (2014, 2015). Also from those spectroscopic analyses, we reckon that the contamination in the rest of our unconfirmed HAEs is less than 10 per cent. This protocluster core contains four very dense groups of HAEs: one in the immediate vicinity of the radio galaxy (RG), two towards the south-west (the further one is the densest) and one to the north of the RG (Fig. 2b). Within the MOIRCS survey field, we identify significant Lyα emission lines for nine HAEs including the RG that meet our LAE criteria. We also find four more objects that have both Lyα and Hα detections in the two narrow-bands, which were deselected from our original HAE samples in Hayashi et al. (2016) by their colour–colour criteria. Including those, 104 HAEs are now identified in total as protocluster members, and 13 of those are also classified as LAEs. On the other hand, three LAE candidates show

[1] http://irsa.ipac.caltech.edu/applications/DUST/

[2] The bandpass of NB428 for Lyα does not perfectly match that of NB2315 for Hα. This leads to a 10 per cent Lyα flux loss on average for HAEs, which is considered in our stacking analyses (Section 4). Also, the NB2315 bandpass shifts bluewards towards the edge of the MOIRCS field of view; however, this effect can be negligible for our HAE samples according to previous follow-up spectroscopy (Shimakawa et al. 2014). Furthermore, NB428 covers redshifts higher by $\gtrsim$1500 km s^{-1} for Lyα with respect to NB2315 for Hα, and, thus, a possible redwards velocity offset of Lyα relative to Hα (Shapley et al. 2003) would be negligible.

Downloaded from https://academic.oup.com/mnrasl/article/468/1/L21/3060937 by guest on 10 April 2024

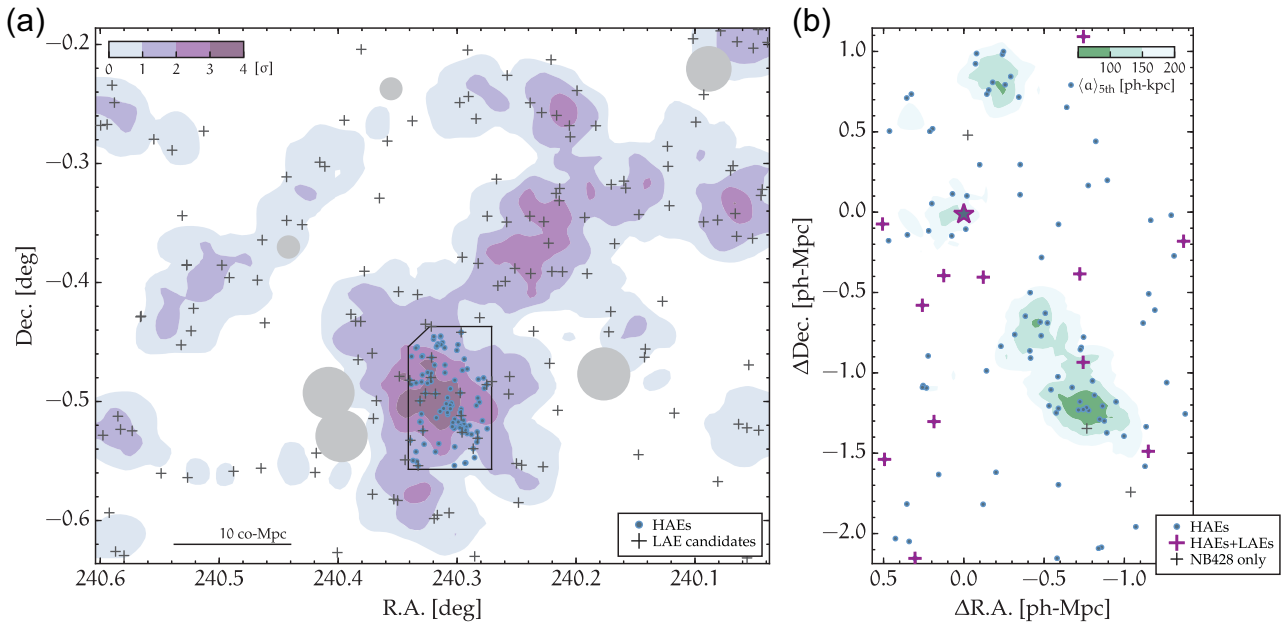

Figure 2. 2D maps of the USS 1558 protocluster with Suprime-Cam (a) and MOIRCS (b). (a) The black crosses represent the LAE candidates and the blue circles indicate the HAEs identified by Hayashi et al. (2016). The filled contours indicate the significance of LAE overdensities (0–σ, σ–2σ, 2σ–3σ and 3σ–4σ), which are smoothed by the Gaussian kernel of $\sigma = 1$ degree. The region enclosed by the black lines corresponds to the survey field of MOIRCS for HAEs. (b) The symbols are the same as in (a), but the purple crosses show the dual Hα and Lyα emitters. The star symbol indicates the RG. The filled contours show the mean distance of, 200–150, 150–100 and <100 ph-kpc, smoothed by the Gaussian kernel of $\sigma = 0.5$ arcmin.

no Hα emission line in our previous narrow-band imaging in the near-infrared. Some of these are likely to be foreground contaminations (emitters of other than Lyα) and the rest would be faint HAEs.

The LAE density map shows a 4σ excess peak traced by HAEs just around the main body of the protocluster USS 1558. A notable LSS or gigantic filament extends towards the north-west. Follow-up spectroscopy is needed to confirm the structures since our LAE samples may contain other foreground line contaminations. Surprisingly, however, on a much smaller scale [$\sim$300 ph-kpc (physical kpc)], HAEs with Lyα line detections are distributed as if they are trying to avoid the overdense groups of HAEs (Fig. 2b). It is remarkable that there is no LAE except for the RG in any of the notable dense group cores of HAEs in spite of the 4σ overdensity in LAEs in this protocluster as a whole on a $\sim$10 co-Mpc (comoving Mpc) scale. To evaluate the deficiency of LAEs in the local overdensities, this work defines a density parameter, the mean projected distance $\langle a \rangle_{N\mathrm{th}} = 2 \times (\pi \Sigma_{N\mathrm{th}})^{-0.5}$ where $\Sigma_{N\mathrm{th}}$ [$= N/(\pi r^2_{N\mathrm{th}})$] is the number density of HAEs within the radius $r_{N\mathrm{th}}$, which is the distance to the $(N-1)$th neighbours from each HAE. We use $N = 5$. We stress that this density parameter maintains a relative consistency even if we choose different N values.

The median value and the scatter of the mean projected distance ($\langle a \rangle_{5\mathrm{th}}$) is 214^{+140}_{-88} ph-kpc. We investigate the significance of the LAE deficiency in the dense groups by dividing the HAE samples into high-density and low-density sub-samples separated at this median value. The fractions of LAEs among HAEs are 21 ± 11 per cent in the lower densities and only 2 ± 4 per cent excluding the RG (or 4 ± 5 per cent with the RG) in the high-density regions, respectively. Fig. 3 represents the cumulative distributions of $\langle a \rangle_{5\mathrm{th}}$ (a) and stellar mass (b) for the HAEs and the HAEs with Lyα emission detections. The stellar masses of the HAE samples are provided by Hayashi et al. (2016). In (a), the possibility that HAEs and HAEs + LAEs are drawn from the same distribution is only 2 per cent according to the

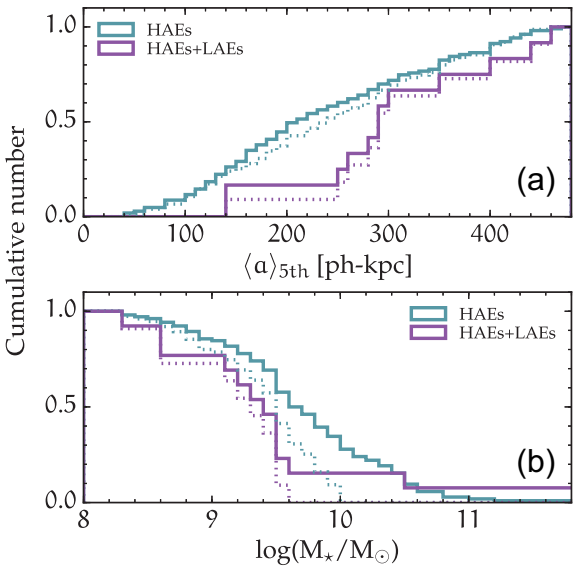

Figure 3. Normalized cumulative distributions of (a) the mean distances and (b) the stellar mass. The blue and purple solid lines indicate the entire HAE samples and HAEs with significant Lyα emission, respectively. The dotted lines show the mass-control sample with $M_\star < 10^{10}$ M$_\odot$.

Kolmogorov–Smirnov test, suggesting that Lyα photons are more depleted in high-density regions. This trend is still statistically significant ($p = 0.04$) even if we use the mass-control samples where we limit the galaxies to only those with stellar masses lower than 10^{10} M$_\odot$. Even if we go further down in stellar masses, where this statistical test would no longer be significant, the LAE deficiency at $\langle a \rangle_{5\mathrm{th}} < 300$ ph-kpc would still remain. In fact, we do not see a significant difference in stellar mass distributions between the HAEs and those with Lyα emission lines; the p value is 0.07 for the entire

Downloaded from https://academic.oup.com/mnrasl/article/468/1/L21/3060937 by guest on 10 April 2024

sample and 0.18 for the mass-control sample, respectively. Such an insignificant or small difference in stellar mass distributions between LAEs and non-LAEs is consistent with recent studies (Hagen et al. 2016; Hathi et al. 2016). We stress that here we employ only the LAEs whose Hα emission lines are detected (as HAEs) by the independent narrow-band imaging in the near-infrared. Therefore, these comparisons are free from the contaminations in our LAE samples, which is a problem only for the LAE-only samples.

4 DISCUSSION AND SUMMARY

Our dual Lyα and Hα line survey of a protocluster at $z = 2.5$ provided us with the first critical insight into the environmental dependence of the Lyα strength compared to Hα. The broad agreement in the spatial distributions between LAEs and HAEs on a large scale ($\gtrsim$10 co-Mpc) indicates that the Lyα line would be a good tracer of LSSs in the high-z Universe. On a smaller scale, however, we see that LAEs, except for the RG, completely avoid the protocluster's dense cores, which are traced by the overdensities of HAEs. This means that LAE surveys of protoclusters would inevitably miss the particularly dense regions of protoclusters, which are likely to be the most interesting and critical environments where we expect to see any early environmental effects, like the progenitors of present-day rich cluster cores. In other words, we are not really able to study environmental effects with the LAEs alone as they can trace only the outskirts of protocluster cores and the larger-scale structures around them. The *James Webb Space Telescope* (Gardner et al. 2006) will be very powerful for searching for truly dense structures at $z > 2.6$ where Hα is no longer available, since it probes the rest-frame optical regime where many nebular emission lines other than Lyα are located. It should be noted, however, that bright Lyα blobs can also be used as a tracer of the central galaxies in massive haloes, as suggested by previous studies (e.g. Steidel et al. 2000; Matsuda et al. 2011).

We measure the escape fraction of Lyα photons by comparing the Lyα and Hα fluxes. This can quantify the deficiency of LAEs in the dense cores of the protocluster and, thus, provide insight into its physical origins. Unfortunately, the current data sets are not deep enough to estimate the escape fraction of Lyα photons for individual HAEs, and, thus, we conduct a stacking analysis and derive the Hα and Lyα luminosities with high precision. The HAE samples are divided into two sub-samples by their local 2D densities at the median value of the fifth mean distance (214 ph-kpc). The narrow-band images are then combined with the IMCOMBINE task by median on IRAF.[3] We derive Hα and Lyα fluxes in the same way we measure the individual HAEs and LAEs in Hayashi et al. (2016) and Shimakawa et al. (2017a). Photometric errors are estimated with an approach similar to that taken by Skelton et al. (2014), where the 1σ Gaussian noise in the background counts is measured as a function of variable aperture size. Our error measurements are, thus, performed independently of the SEXTRACTOR photometries since SEXTRACTOR does not consider the pixel-to-pixel correlation and, thus, underestimates the errors, especially for photometries with large aperture sizes. More details of the stacking method and the measurements of fluxes and errors will be presented in a forthcoming full paper (Shimakawa et al. 2017b). We assume 10 per cent flux contamination from the [N II] line to the narrow-band flux for Hα, and 0.7 mag of dust extinction in the Hα flux. The Lyα escape fraction is given by $f_{\rm esc}^{{\rm Ly}\,\alpha} = (f_{{\rm Ly}\,\alpha,{\rm obs}})/(8.7\,f_{{\rm H}\,\alpha,{\rm int}})$ where 8.7 is the ratio of Lyα to Hα under the assumption of case B recombination (Brocklehurst 1971). This work estimates the Lyα and Hα fluxes with various aperture radii from 6 to 30 ph-kpc taking into account that most star-forming galaxies show diffuse Lyα components (Östlin et al. 2009; Steidel et al. 2011; Hayes et al. 2013).

[3] http://iraf.noao.edu

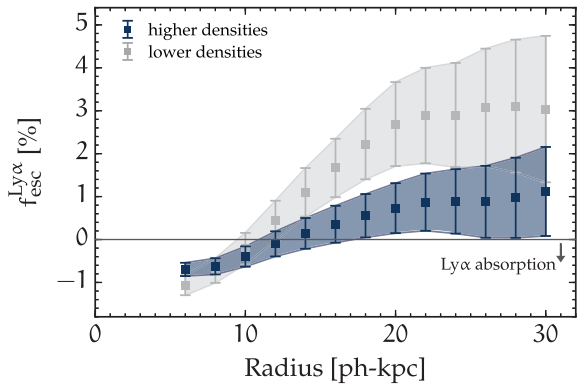

Figure 4. Based on the stacking analysis, the Lyα photon escape fractions ($f_{\rm esc}^{{\rm Ly}\,\alpha}$) of the composite HAEs are shown as a function of photometric aperture radius within which we integrate line fluxes. Here, the HAE samples are split into two sub-samples at the median value of the mean projected distance ($\langle a \rangle_{\rm 5th} = 214$ ph-kpc). The composite HAEs in the higher (lower) density regions are presented by blue (grey) zones, respectively. The error bars represent the photometric errors in the Lyα and Hα line fluxes. The negative $f_{\rm esc}^{{\rm Ly}\,\alpha}$ values mean that Lyα is seen as an absorption line.

We compare the measured Lyα photon escape fractions between the HAEs in high-density regions and those in lower-density regions. Both composite line images seem to have diffuse Lyα profiles, since the escape fraction increases with aperture radius, although photometric errors are quite large. In addition, we see Lyα absorption features within the small aperture radii, which are consistent with the individual detection of Lyα absorption in massive HAEs in the random field (Shimakawa et al. 2017a). Most importantly, we find systematically lower Lyα photon escape fractions for the denser regions. This means that the Lyα emission lines are systematically more depleted in denser regions than in lower-density regions in the protocluster (Fig. 4). However, we should note that the Lyα photon escape fraction is considered to depend on various physical properties, such as dust, SFR and metallicity (Hayes et al. 2010; Matthee et al. 2016), that could depend on the environment. The discrepancy between the two composite HAEs may also contain such secondary factors on top of the environment. Moreover, the narrow-band technique cannot resolve the detailed spectral features around the Lyα line. Thus, our measurements may underestimate the escape fraction due to absorption by the foreground circumgalactic/intergalactic medium (CGM/IGM) (Hayes & Östlin 2006) and/or blue-shifted dense outflowing gas (Reddy et al. 2016).

In summary, we find that LAEs are missing in the dense HAE cores. We also find that the Lyα photon escape fractions in the composite HAEs in the denser regions are lower than those in lower-density regions. In the general field, it is expected that LAEs have less dust and lower H I covering fractions (Shibuya et al. 2014; Reddy et al. 2016) and, therefore, Lyα photons can relatively easily escape from the galaxies. However, in the protocluster core, there is extra surrounding gas and dust components trapped in the group/cluster-scale haloes, which may prevent the Lyα photons from escaping from the systems. Such abundant group-scale H I gas may be supplied from the surrounding regions, for example, by cold

Downloaded from https://academic.oup.com/mnrasl/article/468/1/L21/3060937 by guest on 10 April 2024

streams (Dekel et al. 2009a; Dekel, Sari & Ceverino 2009b). Moreover, since the mean projected distance of HAEs is much smaller ($\lesssim$200 ph-kpc) in higher-density regions than in the lower-density regions, Lyα photons emitted from a HAE have a higher chance of penetrating the CGM associated with other member galaxies in the foreground along the line of sight, and, thus, they may be more depleted. Otherwise, most of the individual galaxies in the dense cores could originally have had lower Lyα photon escape fractions due, for example, to higher dust extinction by a certain environmental effect (Koyama et al. 2013). The current data sets are clearly insufficient to choose conclusively the most plausible explanation (there will be further discussion in Shimakawa et al. 2017b). Deep rest-frame far-UV spectroscopy of the protocluster galaxies with LRIS and/or KCWI on the Keck telescope will be helpful for us to constrain the physical origins of the Lyα depletion effect and to resolve the interplay between protocluster galaxies and CGM/IGM.

ACKNOWLEDGEMENTS

The data were collected at the Subaru Telescope, which is operated by the National Astronomical Observatory of Japan. This work is subsidized by the Japan Society for the Promotion of Science (JSPS) KAKENHI grant 15J04923. This work was also partially supported by the Research Fund for Students (2013) of the Department of Astronomical Science, SOKENDAI. We thank the anonymous referee for useful comments. RS and TS acknowledge support from JSPS through research fellowships for young scientists. TK acknowledges KAKENHI grant 21340045.

REFERENCES

Bertin E., Arnouts S., 1996, A&AS, 117, 393
Brocklehurst M., 1971, MNRAS, 153, 471
Cappellari M. et al., 2011, MNRAS, 416, 1680
Chabrier G., 2003, PASP, 115, 763
Cole S., Lacey C. G., Baugh C. M., Frenk C. S., 2000, MNRAS, 319, 168
Dekel A. et al., 2009a, Nature, 457, 451
Dekel A., Sari R., Ceverino D., 2009b, ApJ, 703, 785
Dressler A., 1980, ApJ, 236, 351
Fitzpatrick E. L., 1999, PASP, 111, 63
Gardner J. P. et al., 2006, Space Sci. Rev., 123, 485
Hagen A. et al., 2016, ApJ, 817, 79
Hathi N. P. et al., 2016, A&A, 588, A26
Hayashi M., Kodama T., Tadaki K.-I., Koyama Y., Tanaka I., 2012, ApJ, 757, 15
Hayashi M., Kodama T., Tanaka I., Shimakawa R., Koyama Y., Tadaki K.-I., Suzuki T. L., Yamamoto M., 2016, ApJ, 826, L28
Hayes M., Östlin G., 2006, A&A, 460, 681
Hayes M. et al., 2010, Nature, 464, 562
Hayes M. et al., 2013, ApJ, 765, L27
Kajisawa M., Kodama T., Tanaka I., Yamada T., Bower R., 2006, MNRAS, 371, 577
Kodama T., Tanaka I., Kajisawa M., Kurk J., Venemans B., De Breuck C., Vernet J., Lidman C., 2007, MNRAS, 377, 1717
Koyama Y. et al., 2013, MNRAS, 434, 423
Matsuda Y. et al., 2011, MNRAS, 410, L13
Matthee J., Sobral D., Oteo I., Best P., Smail I., Röttgering H., Paulino-Afonso A., 2016, MNRAS, 458, 449
Miyazaki S. et al., 2002, PASJ, 54, 833
Oke J. B., Gunn J. E., 1983, ApJ, 266, 713
Östlin G., Hayes M., Kunth D., Mas-Hesse J. M., Leitherer C., Petrosian A., Atek H., 2009, AJ, 138, 923
Ouchi M. et al., 2003, ApJ, 582, 60
Ouchi M. et al., 2004, ApJ, 611, 660
Reddy N. A., Steidel C. C., Pettini M., Bogosavljević M., Shapley A. E., 2016, ApJ, 828, 108
Schlafly E. F., Finkbeiner D. P., 2011, ApJ, 737, 103
Schlegel D. J., Finkbeiner D. P., Davis M., 1998, ApJ, 500, 525
Shapley A. E., Steidel C. C., Pettini M., Adelberger K. L., 2003, ApJ, 588, 65
Shibuya T. et al., 2014, ApJ, 788, 74
Shimakawa R., Kodama T., Tadaki K.-I., Tanaka I., Hayashi M., Koyama Y., 2014, MNRAS, 441, L1
Shimakawa R. et al., 2015, MNRAS, 451, 1284
Shimakawa R. et al., 2017a, MNRAS, tmp, 99
Shimakawa R. et al., 2017b, preprint (arXiv:e-prints)
Skelton R. E. et al., 2014, ApJS, 214, 24
Sobral D. et al., 2017, MNRAS, 466, 1242
Steidel C. C., Adelberger K. L., Shapley A. E., Pettini M., Dickinson M., Giavalisco M., 2000, ApJ, 532, 170
Steidel C. C., Bogosavljević M., Shapley A. E., Kollmeier J. A., Reddy N. A., Erb D. K., Pettini M., 2011, ApJ, 736, 160
Sunyaev R. A., Zeldovich Y. B., 1972, A&A, 20, 189
van Dokkum P. G. et al., 2011, ApJ, 743, L15
Venemans B. P. et al., 2007, A&A, 461, 823
White S. D. M., Frenk C. S., 1991, ApJ, 379, 52
Yagi M., Kashikawa N., Sekiguchi M., Doi M., Yasuda N., Shimasaku K., Okamura S., 2002, AJ, 123, 66

This paper has been typeset from a TEX/LATEX file prepared by the author.

Downloaded from https://academic.oup.com/mnrasl/article/468/1/L21/3060937 by guest on 10 April 2024